ECOLOGY

Spatiotemporal-social association predicts immunological similarity in rewilded mice

Alexander E. Downie[1]†*§ , Oyebola Oyesola[2]†, Ramya S. Barre[1,3], Quentin Caudron[1], Ying-Han Chen[4], Emily J. Dennis[5], Romain Garnier[1], Kasalina Kiwanuka[2], Arthur Menezes[1], Daniel J. Navarrete[1,6], Octavio Mondragón-Palomino[2], Jesse B. Saunders[1], Christopher K. Tokita[1], Kimberly Zaldana[2,7], Ken Cadwell[8,9,10], P'ng Loke[2]‡*, Andrea L. Graham[1,11]‡*

Environmental influences on immune phenotypes are well-documented, but our understanding of which elements of the environment affect immune systems, and how, remains vague. Behaviors, including socializing with others, are central to an individual's interaction with its environment. We therefore tracked behavior of rewilded laboratory mice of three inbred strains in outdoor enclosures and examined contributions of behavior, including associations measured from spatiotemporal co-occurrences, to immune phenotypes. We found extensive variation in individual and social behavior among and within mouse strains upon rewilding. In addition, we found that the more associated two individuals were, the more similar their immune phenotypes were. Spatiotemporal association was particularly predictive of similar memory T and B cell profiles and was more influential than sibling relationships or shared infection status. These results highlight the importance of shared spatiotemporal activity patterns and/or social networks for immune phenotype and suggest potential immunological correlates of social life.

INTRODUCTION

One of the fundamental roles of an organism's immune system is to mediate its interaction with its environment (*1*). Immune phenotypes of humans and other species exhibit considerable nonheritable, environmentally derived variation (*2*–*4*). For example, nonheritable variation in abundance of many types of T and B cells in humans is >80% (*5*). Uncovering which elements of the environment contribute to this variation and how they do so remains an open challenge, crucial both for medical practice (*3*) and for understanding the evolutionary and ecological forces that shape the immune system (*6*).

A key part of an individual's environmental interface is whom they spend time with or interact with and how often. Such patterns of association can shape the transmission and exchange of microbes and antigens, whether pathogenic (*7*, *8*) or nonpathogenic: For example, in the wild, microbiome similarity between individuals correlates with social group membership (*9*, *10*) and the strength of social and spatiotemporal network ties (*11*–*14*). Social interactions are intimately linked to shared spatiotemporal movement patterns because patterns of movement will constrain who individuals interact with, which, in turn, feed back into patterns of movement (*15*–*17*). The two are often treated in the literature as somewhat synonymous, with association networks calculated from spatiotemporal co-occurrences frequently referred to as "social networks" in reflection of these feedbacks. In addition, if socially connected individuals visit similar spaces at similar times, even without physical contact, then individuals could acquire the same antigens preexisting in the environment, beyond any antigen transmission between individuals. This could then be a meaningful force in the observed relationship between social ties and microbiome composition. Spatiotemporal/social connections between individuals are therefore potentially an important influence on antigen exposure and its variation within and among populations.

In turn, antigen exposure strongly influences immune phenotype; exposing lab mice to various symbiotic microbes shapes their immune phenotypes (*18*–*20*), while systematic enrichment of microbiota produces immune phenotypes quite distinct from standard specific–pathogen–free lab mice (*21*–*26*). Other sources of antigens, like allergens, can also influence immune phenotypes (*27*). Thus, mechanisms like common antigenic experience through microbial/allergen transmission or shared environmental acquisition of antigens could create correlative, and possibly even causal, links between spatiotemporal/social networks and immune phenotypes. For instance, long-term space use patterns have been shown to be correlated with immune phenotype in red deer (*28*). Ties between elements of an individual's sociality and immune phenotype have been previously identified in mice; for example, tumor necrosis factor–α (TNF-α) levels have been associated with gregariousness (*29*), while interleukin-17 receptor A (IL-17RA) and

[1]Department of Ecology and Evolutionary Biology, Princeton University, Princeton, NJ 08544, USA. [2]Laboratory of Parasitic Diseases, National Institute for Allergy and Infectious Diseases, National Institutes of Health, Bethesda, MD 20892, USA. [3]Department of Microbiology, Immunology, and Molecular Genetics, University of Texas Health Sciences Center at San Antonio, San Antonio, TX 78229, USA. [4]Kimmel Center for Biology and Medicine at the Skirball Institute, New York University Grossman School of Medicine, New York, NY 10016, USA. [5]Janelia Research Campus, Howard Hughes Medical Institute, Ashburn, VA 20147, USA. [6]Department of Microbiology and Immunology, School of Medicine, Stanford University, Stanford, CA 94305, USA. [7]Department of Microbiology, New York University Grossman School of Medicine, New York, NY 10016, USA. [8]Division of Gastroenterology and Hepatology, Department of Medicine, University of Pennsylvania Perelman School of Medicine, Philadelphia, PA 19104, USA. [9]Department of Systems Pharmacology and Translational Therapeutics, University of Pennsylvania Perelman School of Medicine, Philadelphia, PA 19104, USA. [10]Department of Pathology and Laboratory Medicine, University of Pennsylvania Perelman School of Medicine, Philadelphia, PA 19104, USA. [11]Santa Fe Institute, Santa Fe, NM 87501, USA.
*Corresponding author. Email: adownie@princeton.edu (A.E.D.); png.loke@nih.gov (P.L.); algraham@princeton.edu (A.L.G.)
†These authors contributed equally to this work.
‡These authors contributed equally to this work.
§Present address: Department of Primate Behavior and Evolution, Max Planck Institute for Evolutionary Anthropology, Leipzig, Germany.

interferon-γ (IFN-γ) promote neurological disposition toward social behavior (*30*, *31*). In addition, one study has found that co-parenting humans are more immunologically similar to each other than they are to other adults (children were not examined), but it did not consider other social interactions or quantify social networks (*32*). Hence, it remains unclear to what extent and how an individual's immune phenotype is connected to its social life and associations with others, especially the frequency of interactions and identities of the partner(s).

We hypothesize that individuals with stronger spatiotemporal associations should have more similar immune phenotypes. We tested this hypothesis using "rewilded" laboratory mice that are born and raised to maturity indoors in conventional vivaria, then released into outdoor enclosures, where they experience natural weather conditions, eat a varied diet, and have space to roam and burrow. Such settings offer insight into environmental drivers of variation in immune function that are relevant to the natural contexts in which immune systems evolved (*33*), although we did exclude predators and provide chow and water. We used three founder strains of the Collaborative Cross: C57BL/6J, 129S1/SvImJ, and PWK/PhJ. These strains have documented differences in behavior in the lab, such as lower levels of movement in a home cage for 129S1 mice compared to the other two strains (*34*, *35*). Each enclosure contained mice from only one strain; we conducted our experiment in two blocks while rotating strain-enclosure pairings between blocks to decouple effects of genotype and enclosure. We tracked behavior with subcutaneous radio-frequency identification (RFID) tags; five RFID stations per 180-m^2 enclosure—one at the chow feeder and four arrayed in a diamond pattern around the enclosure's perimeter (Fig. 1A)—recorded visits by each mouse during each 5-week experimental period. We collected blood samples for complete blood count (CBC) analysis before release and 2 weeks after release, when we challenged a subset of the mice with *Trichuris muris*, an intestinal nematode parasite. At 5 weeks after release, before any shedding of *T. muris* eggs, we trapped out the mice for extensive immune phenotyping (*36*) and collected fecal samples for microbiome analysis. We analyzed our data using Bayesian linear regression models with appropriate response variable distributions and priors. We generated posterior probability distributions for the associations between predictors and response variables (see Materials and Methods). Our results offer insight into rewilded mouse behavior and reveal intriguing ties between spatiotemporal/social association patterns and immune variation within populations.

RESULTS

Individual and social behavior of rewilded mice varies on several axes

Individual behavior, in terms of the abundance and spatial and temporal distribution of check-ins at RFID stations, varied substantially both within and among strains. PWK/PhJ mice (n = 17) had the most check-ins per night, followed by C57BL/6 mice (n = 23) and then 129S1 mice (n = 20) (Fig. 1B and table S1). PWK/PhJ and C57BL/6 mice traveled similar minimum distances per night but generally further than 129S1 mice (Fig. 1B and table S2). Strain did not predict proportion of check-ins occurring at the feeding station (table S3), but there was wide variation within strains (Fig. 1C). We also observed variation within and among strains in mean roaming entropy, a measure of how evenly spread RFID check-ins are in time and across locations; individuals with more check-ins generally had higher roaming entropy, and C57BL/6 mice had greater roaming entropy than 129S1 mice (Fig. 1D and table S4). In general, strain did influence rewilded mouse individual behavior, but, within a given genetic background, mice still differed substantially (see Supplementary Text).

To study social behavior, we calculated spatiotemporal association networks for each co-housed group based on their appearances at RFID stations. We defined pairwise spatiotemporal association strength with the simple ratio index (SRI), here the ratio of the number of night-location combinations at which the two mice appeared within some defined time interval of each other to the total number of night-location combinations at which one or both mice appeared. For the sake of technical precision we use the term "spatiotemporal association" for this quantity, although it is sometimes referred to in the literature as "social association," and it is often used to quantify animal social networks (*11*, *16*, *37*, *38*). Using spatiotemporal overlaps for mapping said social networks can be preferable to relying solely on physical interactions (*16*), partly because interactions between individuals may be visual, aural, and/or olfactory, not simply physical. Thus, spatiotemporal association may be very informative for studying social behavior. However, there are complexities in the precise relationship between social connections and shared spatiotemporal behavior patterns, and often the two cannot be readily separated, especially given their mutual feedbacks (*15*).

Much like individual activity, observed spatiotemporal associations varied within and among strains. C57BL/6 mice and PWK/PhJ mice both had stronger pairwise associations over 15-min overlap windows than 129S1 mice (n = 290) (Fig. 2A, table S5, and fig. S1). PWK/PhJ and C57BL/6 mice had similar average pairwise association strengths despite PWK/PhJ mice having many more check-ins than C57BL/6 mice (Figs. 1B and 2A). Together, these results suggest that stronger pairwise spatiotemporal associations are not simply or even necessarily a product of more RFID check-ins. Furthermore, neither sibling relationships nor cage-sharing before release influenced association strengths (fig. S2 and table S5). Associations were stronger at feeding stations than at nonfeeding locations for all strains, but mice did associate at nonfeeding locations (mean strength of social associations at nonfeeders across all three strains= 0.196) and pairwise associations at the two sets of locations were correlated (Pearson's r = 0.524) (Fig. 2B). Intriguingly, despite the variation in pairwise association strength, within each enclosure's network, mice were generally quite similar in their average association strength and centrality (fig. S3). The challenges with *T. muris* negligibly altered individual and association behavior, with the only small effects being slightly decreased check-in counts after infection and a slight increase in the relative proportion of check-ins at the feeder by helminth-infected mice (tables S1 to S6). Overall, we find substantial genetic differences in individual and social behavior in a seminatural setting and further within-strain heterogeneity.

Spatiotemporal association strength positively correlates with similarity of aspects of immune phenotype

We next assessed our hypothesis that immune phenotype and behavior would be linked. We found that individual-level behavior, e.g., number of check-ins, broadly did not predict immune

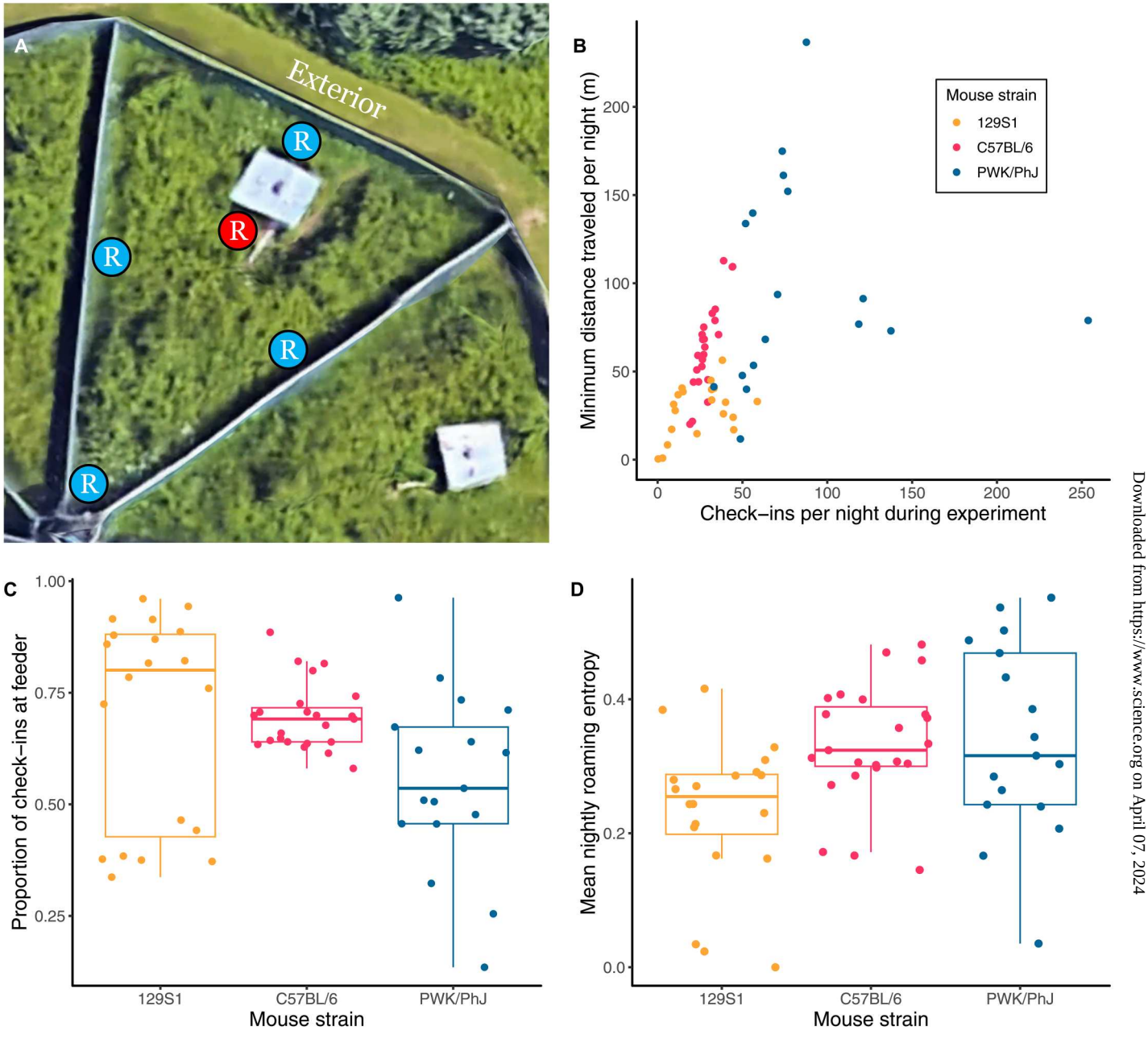

Fig. 1. Rewilded mouse behaviors varied within and among strains. (**A**) Aerial image via Google Earth of one of the three enclosures used during the experiment. "R" circles identify the locations of RFID stations within enclosure (red, chow feeder; blue, nonfeeder); the reader layout was the same for each enclosure, and the three enclosures have similar dimensions. (**B**) Check-ins and minimum distance traveled per night for each individual. The 12 mice that lost RFID tags or moved among enclosures are excluded from plots of individual behavior. (**C**) Proportion of check-ins taking place at the RFID reader attached to the feeding station within each enclosure, for each individual. (**D**) Mean nightly roaming entropy—evenness of RFID activity in time and space—of rewilded mice (see Materials and Methods).

phenotypes of mice, although there were a few exceptions, such as monocyte abundances in the blood negatively correlating with both minimum distance traveled per night and mean roaming entropy (table S7). However, we did find evidence that spatiotemporal associations predicted the immune phenotypes of the mice. We calculated pairwise similarities for each of several aspects of immune phenotype at the time of trapout: white blood cell profiles drawn from CBC measurements, CD4, CD8, and combined CD4 and CD8 T cell memory phenotypes (determined from cell surface expression of CD44 and CD62L as measured by flow cytometry) in blood and mesenteric lymph nodes (MLNs), B cell CD44 and CD62L expression phenotypes in the MLNs drawn from flow cytometry, plasma cytokine concentrations, and MLN cytokine production from antigenic stimulation (*36*). To quantify pairwise similarity, we used Jaccard index for cell-type distributions and Manhattan distance for cytokine measures. Using multiple-

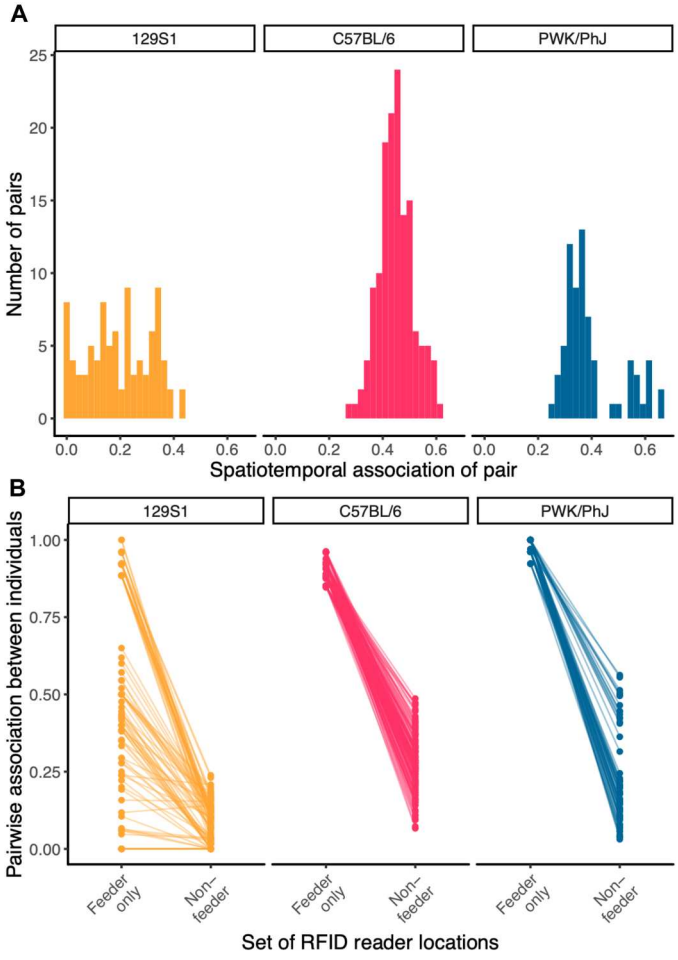

Fig. 2. Rewilded mouse pairwise association levels varied within and among strains and locations. Pairwise associations for this plot were calculated from spatiotemporal co-occurrences with a 15-min overlap threshold. (**A**) Strength of social associations for each pair of mice, broken down by strain. (**B**) Pairwise social association strengths, broken down by strain, by set of locations considered: only associations at RFID reader at feeding station ("Feeder only") versus only associations at all other RFID readers ("Nonfeeder").

membership mixed-effects Bayesian linear regressions, we found that strength of spatiotemporal association of a pair of mice correlated positively with pairwise similarity of several aspects of their immune phenotypes, in that the values of regression-estimated coefficients for the relationship between a pair's spatiotemporal association and immune phenotype similarity are largely or entirely positive. This relationship was strongest for CD4 T cell memory phenotypes in the MLNs (n = 362 pairs), but combined MLN CD4/CD8 T cell memory (n = 362), MLN B cell phenotypes (n = 362), and white blood cell profiles from CBC differentials (n = 391) also exhibited positive correlations between spatiotemporal association and immune similarity (Fig. 3, A and B; fig. S4; and table S8). We did not find relationships between spatiotemporal association and similarity of blood T cell (n = 323) or plasma cytokine profiles (n = 306); intriguingly, similarity of in vitro MLN cell cytokine production in response to stimulation showed a negative correlation with spatiotemporal association strength (n = 147) (Fig. 3, A and C, and tables S8 and S9). In addition to the relationship with spatiotemporal association, we consistently found that different strains exhibited different levels of immune similarity; shared infection status (i.e., both helminth-infected or both uninfected) often had a small positive effect on immune similarity, while sibling relationships consistently had none (Fig. 3B and tables S8 and S9). Overall, these results suggest that spatiotemporal association can predict similarity of WBC differentials in the blood and memory lymphocyte composition in lymphoid tissue.

We next used CBC data from blood draws taken at three time points—before release, the midpoint at 2 weeks after release, and the endpoint at 5 weeks after release—to examine how the relationship of immune similarity to spatiotemporal association changed across the experiment. Immune similarity before release only weakly correlated with immune similarity at the endpoint (Pearson's r = 0.202), with greater CBC variation on average at the end of each block (fig. S6), suggesting that mouse immune phenotypes changed significantly during the experiment, increasing in variation [see (*36*) for more discussion of temporal variation in CBC profiles]. We found that pairwise CBC similarity before release did not predict spatiotemporal association during the experiment. We then observed weak signs of a correlation between midpoint CBC similarity and spatiotemporal association (Fig. 4A and table S10), but, by the experimental endpoint, we observed an appreciable relationship between CBC similarity and spatiotemporal association. Accordingly, our data suggest that the relationship between immune similarity and spatiotemporal association was not preexisting, nor did early immune similarity prefigure which spatiotemporal associations developed. Rather, this relationship emerged during the experiment, raising the possibility that the spatiotemporal associations between individuals structured the immunological changes developing during the release period.

Multiple mechanisms may link spatiotemporal association and immune similarity

We found that pairwise immune similarity was positively correlated with spatiotemporal association in our rewilded laboratory mice, and this relationship emerged during the period of rewilding. These results indicate a form of network assortativity (*39*): Mice that associated more had more similar immune phenotypes. Several non-mutually exclusive mechanisms could underlie this relationship. Spatiotemporal association could be a proxy for direct or indirect microbial transmission between individuals, similar environmental acquisition of antigens (*40*, *41*), and/or shared dietary proclivities (*42*, *43*). Using environmental covariates and different types of spatiotemporal association patterns, we can investigate these possible mechanisms underlying the observed relationship.

A key potential mechanism underlying our observed relationship would be if spatiotemporal association networks facilitated transmission, exchange, or acquisition of microbes, allergens, and other antigens that shape immune phenotypes. Such antigens could be transmitted directly, transmitted indirectly through fomites, coprophagy, or similar routes (*44*), or be in the environment and acquired independently by both individuals. We found no evidence of a range of common mouse pathogens circulating in our rewilded mice (table S11), suggesting that pathogen transmission, which could explain the relationship that we observe, was not taking place. We analyzed fecal microbiome samples from the end of the experiment, using 16S ribosomal RNA (rRNA) sequencing to characterize each individual's microbiome, and examined the

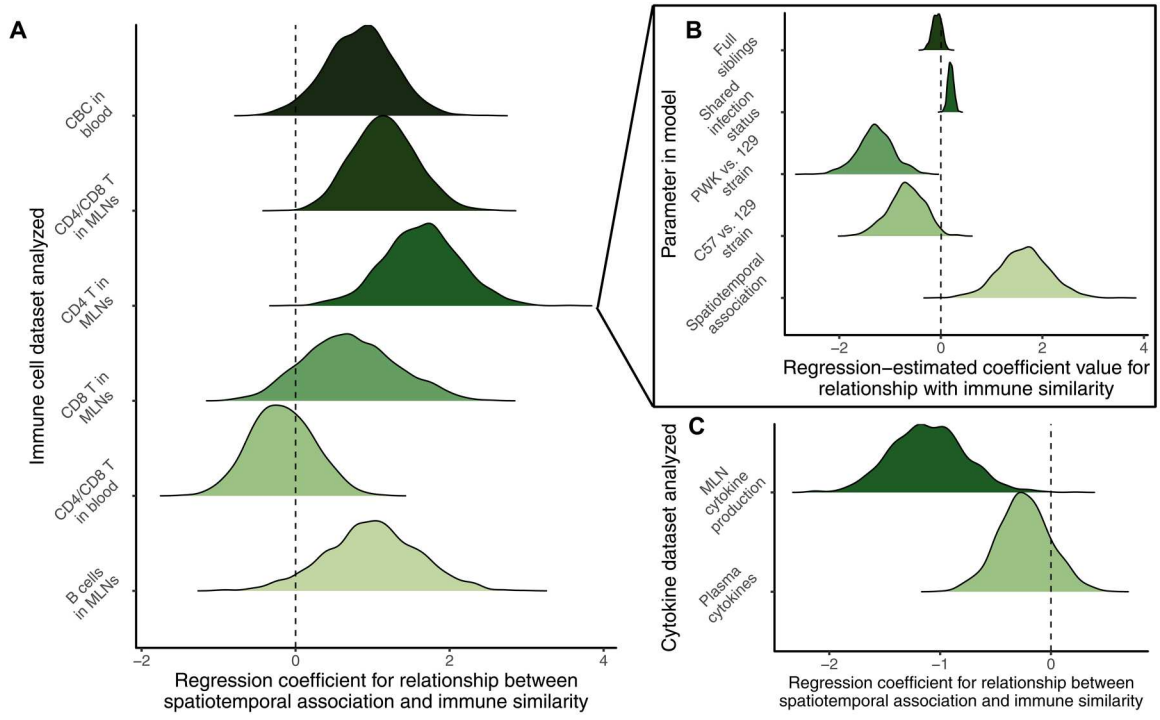

Fig. 3. Spatiotemporal association correlated with immune similarity for several aspects of immune phenotype. Density plots show regression model coefficient posterior probability distributions plotted via 1000 samples from model-estimated coefficient value distribution. Distributions are estimated statistical relationships between parameter in regression and response variable (pairwise similarity of some aspect of immune phenotype). (**A**) Posterior probability distributions for relationship between spatiotemporal association and cellular immune similarity, estimated by Bayesian linear models. Other predictor variables in models were strain of dyad, shared infection status, and sibling relationships; individual identity was included as a random effect. See numerical statement of plotted results in table S8. (**B**) Full model results for fixed-effect predictors from the model of CD4 T cell memory phenotype similarity in mesenteric lymph nodes (MLNs) included in (A). Distributions scaled such that the height of the distribution at the point of greatest probability density is approximately equal for each parameter. See numerical statement of plotted results in table S8. (**C**) Posterior probability distributions for relationship between spatiotemporal association and similarity of aspects of cytokine phenotype. See numerical statement of plotted results in table S9.

relationship between gut microbiome similarity, spatiotemporal association, and immune similarity. We found that pairwise spatiotemporal association strengths did not correlate with similarity of gut microbiota (n = 338) (table S12). Furthermore, we did not find evidence of a relationship between microbiome similarity and immune similarity for CD4 T cell memory phenotype in the MLNs (n = 289) (Fig. 4B), CBC phenotype (n = 315) (fig. S7A), or B cell phenotype in the MLNs (n = 289) (table S13). Our model selection methods preferred models of immune similarity excluding microbiome similarity (table S12). These results suggest that the gut bacterial microbiome at experimental endpoints is not producing the observed relationship between spatiotemporal associations and immune phenotypes. However, it does not rule out the potential influence of cumulative exposures to microbes or to allergens, and more detailed antigenic experience assessment methods in future studies may reveal relationships between similarity of antigenic experience, immune similarity, and spatiotemporal/social association.

In the meantime, we can use networks calculated in different ways to assess possible routes of common antigenic experience. We compared the predictive powers of networks calculated from four different overlap windows—4 hours, 1 hour, 15 min (our default), and 2 min—and a network calculated by comparing similarity of check-in distributions in space. This last network indicates shared space use without incorporating temporal overlap, while the overlap windows provide varying degrees of strictness in assessing spatiotemporal overlaps. We reasoned that the stronger simple shared space use, without temporal overlap, is as a predictor, the less likely it is that transmission of microbes and antigens is a key driver of the relationship that we observe and the more likely environmental acquisition of microbes is relatively influential. We further reasoned that shorter overlap windows should be more closely tied to direct physical contact, by excluding associations that are not close in time. Space use similarity for a pair of mice correlated well with that pair′s spatiotemporal association as calculated from 15-min overlap windows (Pearson′s r = 0.79) (fig. S8). However, we found that similarity of space use correlated only weakly with CD4 T cell memory similarity in the MLNs (n = 295) (Fig. 4C and table S13) and did not correlate with CBC similarity (n = 295) (fig. S7B and table S14). Instead, we found that associations from all four overlap windows could predict CD4 T cell memory similarity, with 15-min associations being the most predictive but broadly similar predictive power for all four overlap windows (Fig. 4C and table S13). Contrastingly, shorter time intervals appeared more predictive of CBC similarity (fig. S7B and table S14). Our results indicate that simple shared space use is likely insufficient to explain on its own the relationship between spatiotemporal association and immunity and that the temporal aspects of

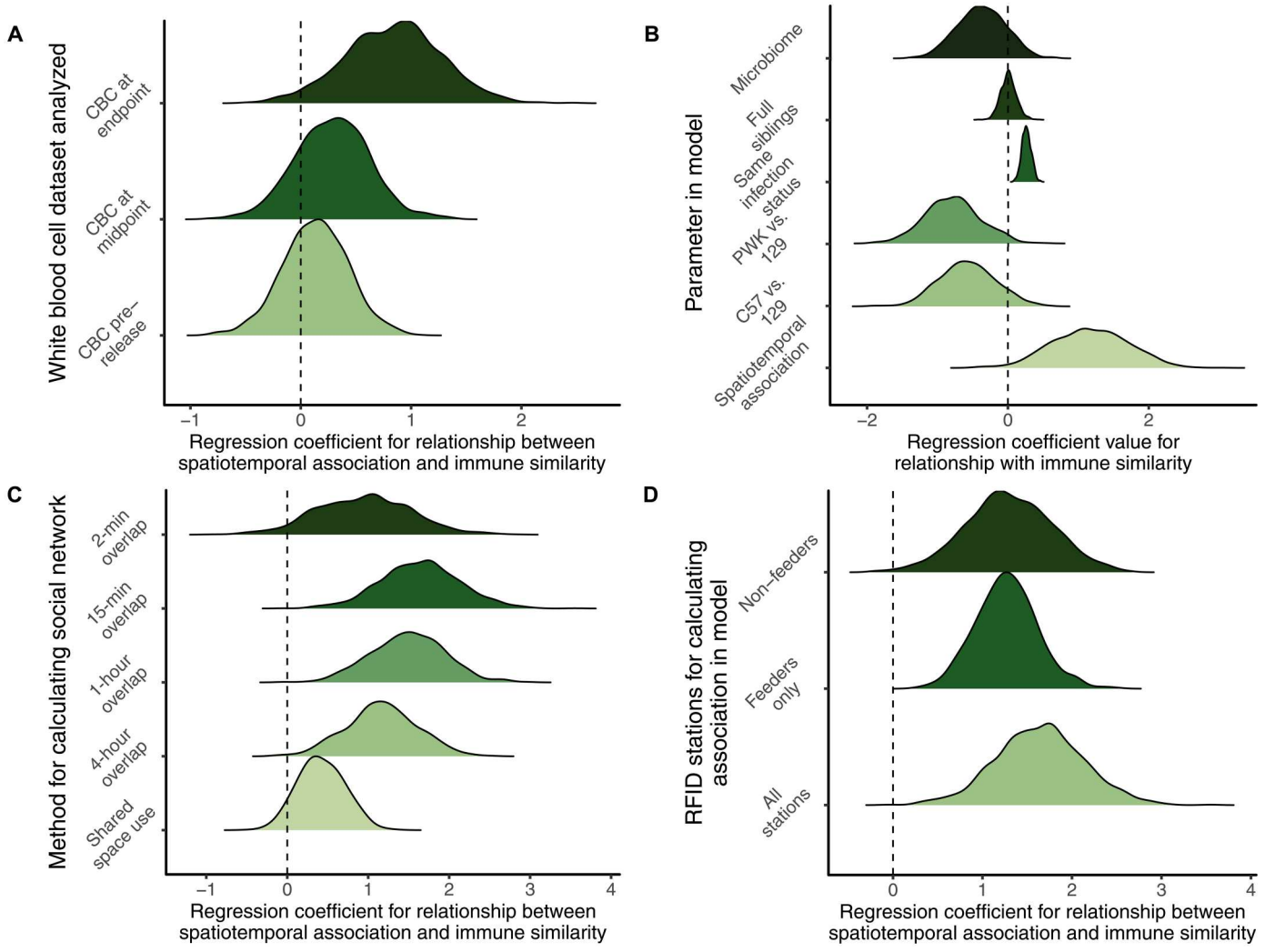

Fig. 4. Exploring hypotheses for the spatiotemporal association–immunity link. Density plots show regression model coefficient posterior probability distributions plotted via 1000 samples from model-estimated coefficient value distribution. Distributions are estimated statistical relationships between parameter in regression and response variable (pairwise similarity of some aspect of immune phenotype). (**A**) Estimated relationships between spatiotemporal association during experiment and similarity of white blood cell profiles (via CBC profiling) at three different time points during experiment. See numerical statement of plotted results in table S10. (**B**) Full results for fixed-effect predictors from model of MLN CD4 T cell memory phenotype similarity in a model that includes gut microbiome similarity. Note that model selection methods do not prefer a model with microbiome similarity over one without. Distributions scaled such that the height of the distribution at the point of greatest probability density is approximately equal for each parameter. See numerical statement of plotted results in table S12. (**C**) Estimated relationships between spatiotemporal association calculated from simple shared space use or from different overlap window lengths and MLN CD4 T cell memory phenotype similarity. See numerical statement of plotted results in table S13. (**D**) Estimated relationships between similarity of MLN CD4 T cell memory phenotypes and spatiotemporal association calculated from different subsets of RFID readers. See numerical statement of plotted results in table S15.

spatiotemporal associations between individuals are crucial. Furthermore, our results suggest that closer temporal windows in spatiotemporal association may be particularly influential for some aspects of immune phenotype, such as the myeloid cells (monocytes, neutrophils, etc.) that appear in our CBC dataset but not our flow cytometry dataset.

One other factor that could produce the observed statistical relationship is dietary similarity. Because diet can influence immune phenotypes (*42*, *43*), shared diets could drive immunological similarity. We do not have precise dietary data, so we cannot properly test this hypothesis. However, we reasoned that spatiotemporal association at the feeding station may be relatively more predictive of dietary similarity than association at nonfeeding stations because it indicates shared use of a known food resource. We compared how association at feeding stations versus nonfeeding stations predicted immune similarity. We found that nonfeeder and feeder associations predicted CD4 T cell memory similarity approximately equally well (Fig. 4D and table S15), while nonfeeder associations predicted CBC similarity better than did feeder associations (fig. S7C and table S16). These results are consistent with dietary similarity not being a key driver of immune similarity, but it offers only a preliminary insight, and more detailed analysis of diet in future studies will be necessary to investigate this possibility further.

DISCUSSION

We report a previously unidentified relationship between an organism's association network and its immune phenotype. Individuals that spatiotemporally associate more often are more similar in immune phenotype than individuals who do not associate frequently. These effects are not present for all cell types in all tissues, but they are particularly strong for lymphoid cell memory phenotypes in lymphatic tissue, where antigen recognition takes place. Environment is a major contributor to immune variation, especially adaptive immune variation (*2*, *3*, *5*). The rewilding system, by providing scope for extensive variation in behavior and microbial environment, allows us to begin to unpick the role of shared spatiotemporal behavior patterns, social behavior, and common antigenic experience, as important mediators of this emergent, nonheritable immune variation. Adaptive immune similarity among spatiotemporal associates has important epidemiological and evolutionary implications, addressed below.

The relationship we observe between spatiotemporal association and immune cell similarity is most consistent with social and/or spatiotemporal behavior shaping the immune phenotypes, rather than immune phenotypes driving the observed behaviors. There are three reasons for this. First, we generally do not observe correlations between the abundance of individual immune cell types and a mouse's behavior, as would occur in the latter case. Second, the similarity of CBC phenotypes before release into the enclosures does not predict the strength of spatiotemporal association between pairs of mice, which we would expect if immune phenotypes prefigured behavior. We can predict how similar two mice will be in their immune phenotypes by examining their spatiotemporal associations over the preceding 5 weeks; we cannot predict how often a pair will associate over the next 5 weeks by examining initial immune phenotypes. Third, the fact that the observed relationship is strongest for adaptive immune cells suggests that the experience of specific antigens, which would particularly be influenced by differences in association, is especially important for this relationship. This result is more consistent with social behavior, or some mechanism linked to spatiotemporal/social association, shaping immune similarity than with immune similarity shaping social behavior.

There are several plausible mechanisms for the emergence of a relationship between spatiotemporal and immune phenotype that deserve closer study. A simple rationale for why such association would predict similarity of immune phenotype is that individuals that associate more have more similar antigenic experiences. Individuals could acquire the same antigens directly from the environment or from each other by direct contact or indirect transmission from fomites, coprophagy, etc., with this latter route not requiring individuals to be in the same place at the same time. Similar diets could also produce some similarity in antigenic experience and could also directly affect immune phenotype (*43*). Our analyses do not lend particular support to any of these mechanisms. It is especially noteworthy that the similarity of gut microbiota, as assessed by 16*S* rRNA sequencing, does not correlate with either spatiotemporal association patterns or with immune similarity, as we might expect if organisms were transmitting microbes to each other or if individuals were acquiring the same environmental microbes through spatiotemporal co-occurrence. Relationships in the wild between social/spatiotemporal associations and microbiome similarity are particularly well-recorded in the literature (*14*). However, our mice start in the lab with a relatively homogeneous microbiome, unlike in the wild, at least within each strain. Their range is relatively restricted, and, importantly, all mice use the feeder at least occasionally, meaning they have common dietary components and a specific location that could easily homogenize microbiota without requiring close spatiotemporal association. This would obscure a relationship of microbial similarity with both immune phenotype and spatiotemporal association. Other techniques for assessing gut microbiome may be required because our methods may not reveal important fine-grained distinctions among bacteria (*45*). We did not find any evidence of common mouse pathogens spreading in our mice either, suggesting that infections are not underlying our observations.

Despite this ambiguity, we suspect that shared antigenic experience is the most likely explanation for our observations. Several of our results buttress this claim. First of all, as previously mentioned, the strongest correlation with spatiotemporal association is in similarity of adaptive immune cell phenotypes in the MLNs; these cells are therefore located in key sites of antigen presentation and change phenotypes in response to gastrointestinal (GI) antigens. Furthermore, our analyses also do not encompass the fullness of antigenic exposure. For example, fungal microbiota, which have been shown in the past to influence the immune phenotypes of both rewilded and laboratory mice (*24*, *46*), and the virome could also be influencing immune phenotype. We only assess the gut bacterial microbiome here, but there may be important antigens in the skin or oral microbiota that are influencing immune phenotypes. Another nuance is temporal: The gut microbiome is quite variable with time, while immune phenotypes, particularly memory phenotypes, may be relatively stable records of aggregate experience over a long timeframe. Thus, the gut microbiome as measured at any given point in time may not accurately convey the sum of antigenic experience shaping the immune system. An additional explanation for our results would be that social cues and behaviors themselves might underlie the similarity of immune phenotypes. However, we see relatively little evidence that we can predict immune phenotypes from individual behavior profiles, and, while social cues like observing sickness in others can shape immune phenotype (*47*), they have not been documented as causing convergence per se. Further investigation is needed to quantify the relative contributions of direct and indirect transmission of microbes to antigenic exchange between spatiotemporal and social associates.

We found three immune elements that do not have a positive correlation with spatiotemporal association: blood T cells, serum cytokines, and MLN cytokine production. The lack of a relationship for serum cytokines is expected given that serum cytokines generally are consumed and decay rapidly, on the order of hours (*48*, *49*). This makes them indicators only of very recent immunological dynamics, unlikely to be correlated with long-term association network patterns. The difference between our results for blood and MLN T cells is intriguing, but research in humans has suggested that memory composition in blood and lymphoid tissues often differs strongly within individuals (*50*). Hence, there may be reasons why the relationships would be heterogeneous. Why we observed an association in the MLNs rather than the blood may reflect the importance of MLNs for antigen recognition compared to the blood. The MLNs drain the gut and are where T cells perform antigen recognition on antigens passing through the digestive

system, while the blood is generally not a site of antigen recognition and instead is largely a highway moving lymphocytes between tissues, including lymph nodes (*51*). This distinction in T cell biology in the MLNs versus blood would contrast with the more holistic image of the CBC profiles, a profile more amenable to assessment through peripheral blood because many of the basic leukocyte types are commonly located in the blood.

The negative correlation of spatiotemporal association strength with cytokine production profiles in response to antigenic stimulation is quite intriguing. This would cut against the notion that similar antigenic experiences should produce similar immune phenotypes. However, our past analyses comparing rewilded mice to laboratory mice have suggested that environment has relatively little identifiable effect on cytokine production responses; genetic background instead is a key predictor of the observed variation (*23*, *36*). Antigenic exposure history, as influenced by association patterns, may be less important for this aspect of immune phenotype. Furthermore, the content of social interactions may also have influence here. Social rank, position within a dominance hierarchy, can shape immune phenotype in nonhuman primates, with dominant and subordinate individuals having different immune gene expression patterns both at baseline and in response to antigenic stimulation (*52*–*54*). A similar phenomenon has been identified in lab-housed adult male mice (*55*). Thus, differences in social status may cause divergence in immune phenotype. Because we cannot assess interaction content using our RFID readers, we may be blind to particular elements of behavior that would drive this differentiation among closely associated mice.

The lack of positive correlations between cytokine profiles and spatiotemporal association may be further unexpected given the aforementioned ties of cytokines to neurological disposition toward social behavior (*29*–*31*). Because we saw little variation in the strength of an individual's associations, we cannot properly explore this question. However, the cytokine phenotypes displayed by rewilded mice and their behavior may still be interwoven. Previous rewilding experiments have found that rewilding does produce increases in the magnitude of IL-17 production in response to antigenic stimuli, and this increase may be tied to the increase in granulocytes observed in rewilding and through exposure to commensal fungi, which generally provoke T helper (T_H) 17 cell differentiation (*24*, *36*). Given that IL-17RA mediates neuronal signaling for social behavior, there may be links between type 17 immunity, antigenic experience, and the behavioral variation among rewilded strains described here and observed by others (*17*). We might also particularly expect variation between lab-housed and rewilded mice in their degree of sociability because of their differences in IL-17 signaling (*30*). Other cytokines, like TNF-α (*29*) and IFN-γ (*31*), may produce similar effects. Investigations in rewilded mice and comparisons with lab mice can offer greater insight into the links between immunity, neurobiology, and behavior and the multivalent pressures on this relationship.

Further research can help to disentangle the relative contributions of social ties, shared spatiotemporal activity, common antigenic experience, diet, and other factors to the statistical relationship that we observed here. One approach, to investigate the influence of commensal symbionts, would be simply to characterize microbiota in greater depth, using metagenomic sequencing approaches (*14*, *45*), samples from different tissues with different microbiotas (e.g., skin), and more samples across the duration of the experiment, to better grasp fine-grained distinctions in microbial communities at the endpoint and longitudinally. Labeled microbes (*56*) could allow assessment of microbe transmission/sharing within networks, probing the relative frequency of antigen transmission versus shared acquisition from the environment. Characterizing diet during a rewilding period would allow a direct inquiry into the role of dietary similarity in immune similarity, as well as identifying whether association patterns do correlate with shared diets. An alternative way to investigate the mechanisms producing the behavior-immunity relationship seen here would be through reductionist experiments in laboratory settings. For example, using arenas that are sequentially visited by individual mice would remove the possibility for physical contact while still allowing mice to share space in close temporal proximity and therefore acquire the same antigens from the environment [although they may also transmit them indirectly to each other (*44*)]. Laboratory experiments with greater control over initial microbiota could also identify mediating effects from microbes on changes in immune phenotype with time and reactions to antigenic experience. In addition, laboratory experiments in large cages with opportunities for social contact, as in (*55*, *57*), would retain overall variation in interaction while controlling diet. They can also allow fuller tracking of activity via video to identify with greater precision social networks and physical contacts for closer investigation of how different types of association might contribute to immune phenotype similarity.

Regardless of the precise mechanism(s) underlying the relationship between immunological similarity and spatiotemporal association, these results offer intriguing insight into the flexibility of the immune system in response to new conditions and experiences. As previously noted, immunity-behavior relationships like those that we observe here may generate and structure some of the extensive heterogeneity observed in human immune phenotypes (*2*, *3*). Our observations help explain the previously identified immunological similarities between co-parenting humans (*32*), by showing that frequent associations between individuals, as would occur when co-parenting, produce higher immune similarity, while revealing a broader influence of interaction patterns on immune variation. Moreover, if spatiotemporal association influences immune state and if immune state can predict functional responses (*3*, *25*), then individuals that are more associated should be more similar in their susceptibility to a given parasite challenge, at least in some aspects of the immune response, e.g., memory quality and specificity, if not others, e.g., cytokine responses. Heterogeneities in disease susceptibility have been shown theoretically and empirically to affect infectious disease dynamics and pathogen evolution (*58*, *59*). Our work here highlights a way that such heterogeneities might emerge and may therefore identify a phenomenon important not only for hosts but also for pathogens.

Overall, we document extensive behavioral variation in laboratory mice rewilded in outdoor enclosures. We show that interactions between individuals link with immune phenotypes such that the more associated two individuals were, the more similar their immune phenotypes were. This effect, which emerged during the experiments, was particularly strong for cellular composition but weak or even negative for cytokines. These results offer intriguing implications for the generation of natural immune variation and the role of social and spatiotemporal contact in shaping immune systems, and they highlight important new directions of study for

understanding disease susceptibility, infectious disease ecology, and the operation of natural selection on immune phenotypes.

MATERIALS AND METHODS

Rewilding

For our rewilding, we used n = 89 female mice from three mouse strains used as founders of the Collaborative Cross: C57BL/6, 129S1, and PWK/PhJ. Genetic variation in these strains spans ~50 million single-nucleotide polymorphisms, a similar order of magnitude to the total variation documented among humans (*60*, *61*). The experiment took place across two consecutive blocks. Before each block, mice were bred at the National Institutes of Health before shipping to Princeton University for acclimation in a dedicated animal facility to temperatures and light cycles characteristic of summer in New Jersey (26° ± 1°C and a 15-hour light/9-hour dark cycle). Mice were housed in cages of five before release; a subset of mice from each cage was chosen for release, while the others were kept as controls in the warm and humid vivarium (*36*). For release, the mice were divided into three groups per block, with each group consisting of a single strain. In block 1, we released n = 42 mice (15 PWK/PhJ, 14 C57BL/6, and 13 129S1); in block 2, we released n = 47 mice (16 PWK/PhJ, 18 C57BL/6, and 13 129S1). Strains were kept separate to avoid any potential for antagonistic interactions, and, between blocks, we rotated the enclosure to which each strain was assigned so that enclosure pen and mouse strain were unconfounded. All experimental procedures were approved by the Princeton University Institutional Animal Care and Use Committee (protocol no. 1982).

We placed each group of mice in a set of enclosures located in Princeton, New Jersey, during the late spring and summer of 2021. Block 1 ran from May to June 2021, and block 2 ran from July to August 2021. These enclosures (fig. S1), described in (*21*) and also used in (*23*, *24*, *26*, *42*), are triangular wedges, ~180 m^2 in area, and enclosed by 1-m-high walls of zinc-coated steel, which penetrate into the ground of ~0.5 m. Natural vegetation grows in the wedge, with the exception of a strip around the perimeter of the enclosures, which is kept clean-cut for access, and there is a low wooden hut of 180 cm by 140 cm by 70 cm with a corrugated metal roof that provides some shelter. The exterior walls are topped with an electric fence to exclude any terrestrial predators or other animals, while aerial predators are deterred with the expedient of several fishing lines strung over each enclosure and hung with aluminum pie plates. Several years' experiments indicate that these measures are effective at both keeping mice in and predators and other animals out, with the exception of small birds that pose no threat to the mice. Within each enclosure, the mice can roam and forage freely; each enclosure contains one feeding station near the hut stocked with lab chow (PicoLab Rodent Diet 20) and two water bottles inside the hut. We checked the status of these three times a week, topping up the chow if necessary and completely replacing it each week and refilling the bottles if they were running low.

We tracked mouse behavior via RFID check-ins. Before release, we injected each mouse with a subcutaneous RFID tag (8 mm–by–1.4 mm FDX-B "Skinny" PIT Tag, Oregon RFID, Portland, OR, USA), patched the injection site with liquid bandage, and allowed the mouse time to heal. Each enclosure contained five RFID readers, of a design described by Budischak *et al.* (*42*). Briefly, each reader consisted of a plastic PVC tube ~45 cm in length around which an antenna, connected to an RFID reader/writer, is wrapped. When a mouse runs through the tube, the RFID reader/writer records the tag number of that mouse and transmits it to a central database that records the tag number, the particular RFID reader, and the date and time of the check-in (see further details below). One of the five RFID readers in each enclosure was attached to the feeding station, such that each time the mouse entered or exited the feeding station, it produced a check-in. The other four were arranged in a diamond pattern around the perimeter of the enclosure (Fig. 1A).

Before shipping from the breeding facility, blood samples for CBC analysis were collected with cheek bleeds; at Princeton, several days before release, fecal samples were collected. At 2 weeks after release, we trapped the mice using Longworth live traps baited with peanut butter and a pellet of lab chow. We placed at least 40 traps in each enclosure, inside and around the hut and in other places throughout the enclosure. We drew further blood samples for CBC analysis and collected fecal samples; we placed blood samples on ice, while fecal samples were immediately placed on dry ice and then frozen at −80°C. We caught n = 6 mice that had lost their original RFID tags since their release into the enclosures; each was given a new RFID tag, and the injection site was patched with liquid bandage. In addition, we selected a subset of individuals (n = 24 for block 1 and n = 27 for block 2) for challenges with *T. muris*, a natural gut nematode parasite of mice. We gave each of these mice 200 embryonated eggs via oral gavage. After sampling and infection challenge, mice were rereleased in their home enclosure. We also caught mice that had escaped from their original enclosure into different enclosures; we returned these mice to their original enclosures and repaired the breach to prevent further escapes.

At approximately 5 weeks after release, we retrapped all mice using the same method. Again, we drew blood samples for CBC analysis with cheek bleeds using a 4-mm Medipoint Golden Rod Lancet Blade (Medipoint NC9922361) and collected fecal samples; then, we anesthetized the mice via isoflurane inhalation and collected the remaining blood with a terminal cardiac puncture for analysis via flow cytometry. We processed the mice for collection of the MLNs, the cecum, and the GI tract. We placed blood samples again on ice, while we placed fecal samples on dry ice and then froze them at −80°C. We dissected the cecum for counts of *T. muris* parasites. In total, at the end of the experiment we recaptured n = 72 of the original 89 mice released.

Immunological assessment

We performed a CBC analysis with differentials of the whole blood sample collected into 1.3-ml heparin-coated tubes (Sarstedt Inc., NC9574345) and analyzed using the Element HT5 Veterinary Hematology Analyzer (Heska), allowing us to ascertain the abundance of leukocytes and the relative abundances of five different leukocyte types (neutrophils, lymphocytes, monocytes, eosinophils, and basophils) in the blood. We assessed lymphocyte populations in the peripheral blood and in the MLNs using flow cytometry.

For blood, whole blood collected via the cheek bleeds into heparinized tubes (Sarstedt Inc., SC MTUBE 1.3ML LI HEP/PK100) was mixed with heparinized blood collected via cardiac puncture method. The combined blood samples were spun for 10 min at 1500 rpm, and plasma was collected and stored at −80°C for further cytokine analysis. The cellular component resuspended in

phosphate-buffered saline (PBS) next underwent a density gradient separation process using the Lymphocyte Separation Media (LSM MP Biomedicals, LLC, Irvine, CA) according to the manufacturer's instruction. Isolated peripheral blood mononuclear cells (PBMCs) were washed twice in PBS and then used for downstream spectral cytometric analysis. Single-cell suspension from the MLNs were prepared by mashing the tissues individually through a 70-μm cell strainer and washed with RPMI. Cells were then washed with RPMI supplemented with 10% fetal calf serum. Live cell numbers were enumerated using the Element HT5 Veterinary Hematology Analyzer (Heska).

For spectral cytometry, single-cell suspensions prepared from the PBMCs and MLNs were washed twice with flow cytometry buffer (FACs Buffer) and PBS before incubating with Live/Dead Fixable Blue (Thermo Fisher Scientific) and Fc Block (clone KT1632; BD) for 10 min at room temperature. Cocktails of fluorescently conjugated antibodies (table S17) diluted in FACs Buffer and 10% Brilliant Stain Buffer (BD) were then added directly to cells and incubated for a further 30 min at room temperature. For the lymphoid panel, cells were next incubated in an eBioscience Transcription Factor Fixation and Permeabilization solution (Invitrogen) for 12 to 18 hours at 4°C and stained with cocktails of fluorescently labeled antibodies against intracellular antigens diluted in the Permeabilization Buffer (Invitrogen) for 1 hour at 4°C.

Spectral Unmixing was performed for each experiment using single-strained controls with UltraComp eBeads (Invitrogen). Dead cells and doublets were excluded from analysis. All samples were collected on an Aurora spectral cytometer (Cytek) and analyzed using the OMIQ software (www.omiq.ai/), and data cleaning and scaling was done using algorithms like FlowCut within the OMIQ software. Subsampled cells including 10,000 live, $CD45^+$ cells were reclustered in an unsupervised version using the Joe's Flow software (Github: https://github.com/niaid/JoesFlow).

We also assessed cytokine phenotypes through two techniques: plasma cytokine levels at time of sacrifice and production of cytokines by MLN cells in response to antigenic stimulus. Plasma concentrations of IL-5, IL-6, IL-22, IL-17A, IFN-γ, and TNF-α were measured also measured using the commercially available murine T_H cytokine LEGENDplex assay (BioLegend) according to the manufacturer's instructions. For MLN cytokine production assays, single-cell suspension of MLN cells were reconstituted in RPMI at 2×10^6 cells/ml, and 0.1 ml was cultured in 96-well microtiter plates that contained ultraviolet-killed microbes (10^7 colony-forming units/ml), 10^5 αCD3/CD28 beads (11456F), or lipopolysaccharide (100 ng/ml) (L2630) or PBS control. The microbes included were *Bacteroides vulgatus* (American Type Culture Collection, 8482), *Candida albicans* (UC820), *Clostridium perfringens* (National Collection of Type Cultures 10240), and *T. muris* excretory-secretory antigens. Supernatants were collected after 2 days and stored at −80°C. Concentrations of IFN-γ, IL-5, TNF-α, IL-2, IL-6, IL-4, IL-10, IL-9, IL-17A, IL-22, and IL-13 in the supernatants were measured using a commercially available murine T_H cytokine LEGENDplex assay (Biolegend) according to the manufacturer's instructions. To quantify the cytokine production, we divided production in response to antigens/microbes by production with 1× PBS and then took the $\log_2$ of the divided quantity plus 1 (to account for any samples with no production in response to antigenic stimulation).

Microbiome

DNA for microbiome analysis was isolated from frozen fecal samples collected at the endpoint using the QIAsymphony PowerFecal Pro DNA Kit (938036) with the QIAsymphony SP instrument. We prepared the DNA library using the SMRTbell Express Template Prep Kit 2.0, and Amplicon-Seq library sequencing was performed on the PacBio Sequel II system. Sequencing reads were primer trimmed, filtered, dereplicated, and then analyzed using the Divisive Amplicon Denoising Algorithm 2 pipeline (https://benjjneb.github.io/dada2/tutorial.html). We performed bacterial taxonomy assignment against the DECIPHER (www2.decipher.codes/Downloads.html). and SILVA v138 databases. We generated an amplicon sequence variant table, which was then used for assessment of pairwise microbiome similarity. We scaled read counts for each taxon for each individual by the total number of reads for that individual, producing relative abundance estimates. From these relative abundance distributions, we calculated microbiome similarity for pairs of mice with Jaccard index.

Individual behavior assessment

We described mouse individual behavior on the basis of RFID visits logged at the five RFID readers in each enclosure. The RFID reader casing houses an RFID reader/writer board (Priority 1 Design) and a Particle Photon Wi-Fi–enabled IoT device (Particle). These are powered with an external power supply plugged in to an outlet at the center of the enclosures. Each time a mouse passes through the RFID reader, the RFID reader/writer transmits the RFID signal to the Photon unit. The Photon unit then transmits to a central Particle server a message containing the RFID number, the reader identity, and the time of the check-in, which is accurate to the second. We collect the data from the Particle server via a webhook in our own database. The resulting behavioral dataset consists of 103,367 check-ins across the two blocks, with RFID number, date, time, and location for each check-in. Each reader was associated with a particular location in its enclosure: the feeder, the left and right sides (relative to the exterior wall of the triangle), base (along the exterior wall), and tower (the reader closest to the tip opposite the exterior wall) (Fig. 1A). We converted each RFID number to the ID number of the associated mouse. Some mice were associated with two RFID numbers because they received replacement RFIDs at the midpoint trapping during the experiment, and we synonymized these RFID numbers in our database.

We applied several filtering steps to ensure that the data did not contain accidental biases. We first identified times when individual RFID readers were offline for an extended period of time, due either to power and Wi-Fi outages at the enclosures or to water entering the reader's casing. If at least one reader was offline during a particular night, then we dropped from the dataset all check-ins from all readers within the same enclosure as the affected reader for the corresponding 24-hour period (12 noon to 12 noon), to avoid misrepresenting spatial location of activity, relative abundance of activity, or social network structure. For our second filtering step, we removed nights during which trapping took place from our check-in dataset, because the number of check-ins for an individual on a given night would depend on when, or if, that mouse entered a trap. In our third step, for each individual that escaped its home enclosure, we also removed from our dataset all of its check-ins taking place outside of the enclosure in which it was initially released. After completion of this filtering, the dataset comprised 97,358 check-ins.

We calculated activity levels using multiple metrics. Because the length of the experiment, in terms of nights of activity, varied from enclosure to enclosure and because some nights had to be removed due to missing reader data, we calculated all activity levels on a per-night basis. In block 1, wedges 2 and 3 have 33 nights of data, while wedge 4 has 25 nights of data; in block 2, wedges 2 and 3 have 26 nights of data and wedge 4 has 27 nights of data (there are fewer nights for block 2 due to a power and Wi-Fi outage that delayed the start of tracking until after release). The simplest metric was the average number of check-ins per night for each mouse. We also calculated average minimum distance traveled and roaming entropy each night. Minimum distance was calculated on the basis of the distances between each RFID reader within a given enclosure. Each time a mouse visited a new reader on a given night, the distance between the new reader and the previous reader was added to the distance that mouse had traveled that night. If the reader visited was the same as the previous reader, then no distance was added. Distances between reader locations varied slightly among enclosures due to differences in overall dimensions. An average across all nights was calculated for each mouse to give the minimum distance traveled per night by that mouse.

Roaming entropy describes how evenly an individual's activity is spread in time and space (*57*). We calculated roaming entropy after the method defined in (*57*), using 12-hour windows, from 8:00 p.m. to 8:00 a.m., corresponding to the hours of greatest mouse activity (fig. S9). The roaming entropy $RE_{i,t}$ for mouse i on day t is

$$RE_{i,t} = -\sum_{j=1}^{k} p_{i,j,t} \log(p_{i,j,t}) / \log(k)$$

where the reader is j and the total number of readers in the wedge is k. $p_{i,j,t}$ is the probability of mouse i being observed at reader j on day t. To calculate this value, we divided each individual night was divided into minute-long windows. For each mouse, the reader most recently visited at the end of that window was assigned as the reader at which the mouse was present during that window (thus assuming that each mouse is in the vicinity of the last reader it visited until it visits a new reader). $RE_{i,t}$ is on the interval [0, 1], with lower values indicating that activity is mostly concentrated at one location and higher values indicating that activity is spread evenly in time around several locations. Mean roaming entropy for an individual was calculated by as the average of their roaming entropies from all nights during which they appeared.

Spatiotemporal association assessment

We similarly assessed social behavior using RFID check-in records. We derived our approach and code from that in (*11*), with suitable modifications for our particular experimental setup; we use the term spatiotemporal association rather than social association to reflect the precise process of calculating associations. The basic metric that we used to calculate pairwise spatiotemporal association strength between individuals is the simple ratio index (SRI). Mice are considered to be associated with each other if they appear at the same location, during a given night, within some time window of each other. SRI for two mice i and j is calculated as

$$SRI = \frac{X}{X + Y_i + Y_j + Y_{ij}}$$

where X is the number of night-location pairs in which the mice overlap at least once during the night; Y_{ij} is the number of night-location pairs in which both mice appear but not within the overlap window; and Y_i and Y_j are the number of night-location pairs in which only mouse i or only mouse j appears, respectively. SRI is bounded on [0, 1], where 0 indicates that individuals never overlap at a location within the given time window, while 1 indicates that, for every night-location pair, they do so at least once. SRI is used in a variety of animal behavior studies and allows us to describe spatiotemporal association patterns among the mice (*11*, *16*, *37*). We calculated association networks for the six different groups—three strains, two blocks. When we use the term spatiotemporal association in our text, we are referring to the associations of pairs of mice as calculated with SRI. We also calculated for each individual an average of the pairwise spatiotemporal association strength for all pairs containing that individual; this is metric is also bounded on [0, 1].

Two major nuances were involved in the calculation of our networks. First, because some mice lost their RFID tags, they did not produce check-in data for periods in which those mice were still active and potentially associating with other mice but did not have an RFID tag. To accommodate these missing data, we implemented an adjustment to SRI calculations for these mice, which we referred to as "time control," again derived from (*11*). For these mice, when determining associations for a pair, we exclude all check-ins taking place after the last night on which the mouse that is recorded with its RFID appeared. This is because the mouse's absence on subsequent nights could plausibly be attributed to loss of its RFID tag, so we are unable to determine whether its partner in the pair was or was not associating with the mouse with the missing tag. To aid this, we identified associations in two discrete chunks, one before the midpoint trapping session and one after the midpoint trapping session, because the midpoint was the time when missing RFID tags were replaced. With this approach, we effectively assume that associations during the phase when the mouse does not have an RFID tag are approximately equal to those occurring at other times of the experiment. Some support for this approach can be found in the fact that, after excluding individuals that lost an RFID tag at some point during the experiment, the strengths of the pairwise associations between pairs of individuals before the midpoint trapping session are well correlated with the strengths of the association after the midpoint trapping session for that pair (Pearson's $r = 0.73$; fig. S9).

The other nuance was in our handling of calculating association strengths for individuals that escaped from their assigned enclosure at some point during the experiment. In these cases, mice would have been physically unable to associate with others in their assigned enclosure. We decided not to excise days of escape from the calculations of association strength for pairs with at least one mouse that escaped from its focal enclosure, because the separation was a genuine factor that altered their frequency of association. Unlike with the lost RFIDs, we do definitively know that the mice of the pair were not associating when one was outside the home enclosure. We did not include escapee mice in the networks of the wedges they entered, however. Thus, all of our associations are between mice that shared home enclosures.

To explore how location and overlap window duration affected estimates of association strength, we calculated networks in several different scenarios. We used four different overlap window lengths:

4 hours, 1 hour, 15 min (our default for presented results), and 2 min. These impose greater or lesser stringency in estimates of association; shorter time frames should be more closely tied to rates of actual contact, simply because associations with these time windows require the mice to be in the same place at a closer time. To investigate similarities in space use independent of temporal overlaps, we also calculated pairwise similarity of check-in distributions. We used the Jaccard index to determine for each pair how similar their distributions of check-ins were across the five RFID reader locations. This statistic tells us how similar individuals were in their patterns of space use, including the abundance of visits to a given location. We did not calculate space use similarity for pairs including individuals that lost an RFID tag, because their check-in profiles were incomplete. We also calculated social networks for subsets of readers: just association at the feeding station in each wedge and association at the nonfeeding stations in each wedge. These allowed us to assess how association strengths varied at different locations. In general, association strengths at different time intervals were correlated with each other, as were association strengths at different sets of locations, but strengths varied on the basis of the length of the overlap windows and the locations included.

Statistical analyses

Our statistical analyses can be broken down into two major subsets: (i) analyses of the relationships between individual immune traits and individual behavior traits and (ii) analyses of the relationship between pairwise immune similarity and spatiotemporal association and other predictors. For all of our statistical analyses, we used a Bayesian framework in R v4.1.2 and the package brms (*62*, *63*). Model selection for each analysis was carried out using widely applicable information criterion (WAIC), a generalized version of Akaike information criterion that can be used with our Bayesian models. The model chosen and presented is that with the lowest WAIC value, except where otherwise specified.

Analyses of individual behavior used mixed-effects linear regression models with appropriate distributions for response variables, as follows. Average check-ins per day and average minimum distance traveled were both log-transformed and modeled as normally distributed response variables. Mean roaming entropy was modeled as a beta-distributed response variable with a logit link function. Immune traits were log-transformed and modeled as normally distributed response variables. For immune trait values of 0 that could not be log-transformed (e.g., basophil concentrations in the CBC), we assigned values immediately below the detection threshold of the assay to ensure that low values for those traits were not systematically excluded from our analyses. Potential fixed-effect variables included for model selection were genotype and infection status, as well as behavioral traits of interest when investigating the effect of behavior on immune phenotypes. Potential random-effect variables were block of the experiment, enclosure in which the mouse was housed, parentage of the mouse, and the cage in which the mouse was housed before release outdoors. For all analyses involving individual behavior either as predictor or response variable, we excluded any mice that either lost an RFID tag or escaped their assigned wedge during the experiment. For analyses of factors predicting pairwise association behavior, we generally used binomial regressions, with the number of trials for each pair of mice being the number of night-location pairs for which at least one of the two mice in the pair appeared and the number of successes being the number of night-location pairs for which the two mice appeared within the designated overlap window.

We took multiple approaches to describing immune similarity as befitting different data. For cell-type abundances, we used methods similar to those used to describe similarity of microbiome composition or species assemblages in community ecology. We assessed the relative abundance of different types of immune cells and calculated the similarity of these abundance distributions as Jaccard index using the R package vegan v2.5-7 (*64*). Jaccard index is on the interval [0, 1], where a value of 0 indicates no overlap at all in the abundance distribution (i.e., entirely dissimilar) and a value of 1 indicates perfect congruence of the abundance distribution (i.e., identical). We calculated similarities in this manner for several different sets of cell types: white blood cell phenotypes from CBC data, combined relative abundances of both CD4 and CD8 T cell memory phenotypes (based on cell-type identity determined from CD62L and CD44 expression on T cells as described above) in each of the peripheral blood and MLNs, as well as just CD4 T cell memory and just CD8 T cell memory in the MLNs, and relative abundance of different B cell phenotypes on the CD62L/CD44 expression axes in the blood and MLNs.

For calculating similarity of cytokine phenotypes, we used Manhattan distance, a metric that determines the cumulative difference along each axis between two phenotypes plotted in an n-dimensional space, where n is the number of traits measured. For plasma cytokines, we first log-transformed the cytokine concentrations so that they were normally distributed and then scaled the resulting values as z-scores, such that Manhattan distance would be the sum of the standard deviations of difference between the two phenotypes across all cytokines. For MLN cytokine production, we adjusted production for null controls as stated above and then followed the same procedure.

The analysis of spatiotemporal/social associations drawn from observation data is considerably more complex and has been the subject of much discussion (*65*–*70*). We opted to use Bayesian multiple-membership mixed-effects linear regressions, which are recognized as a valid statistical approach when analyzing such relationships (*66*, *68*) and for which there are statistical packages capable of handling multiple-member mixed-effects beta regressions (brms, which we use). As above, we used model selection to identify the variables for inclusion in our analyses. Because the response variables were describing the status of a pair, all explanatory variables were chosen to match. Potential fixed-effect variables included were the strain identity of the two members of the pair (with the members of the dyad always of the same strain), whether the individuals were full siblings, and whether the individuals were housed in the same cage before release in their enclosure; spatiotemporal association was also included as a fixed effect in appropriate cases when analyzing immune similarity. We also included infection status, but we used a different treatment of this variable depending on whether we were analyzing social association or immune similarity. When analyzing spatiotemporal association, we used three categories: both mice infected, one mouse infected, or neither mouse infected. When analyzing immune similarity, we used two categories: shared infection status (meaning either both mice were infected or neither mouse was infected) or different infection status. Potential random-effect variables considered included block of the experiment and the enclosure in which the pair were housed, as well as multiple-membership random effects

for each individual in the pair. In general, block, enclosure, and shared parentage were not included in optimal models after model selection, but there were exceptions. Estimated model parameter values are reported and plotted as posterior probability distributions and are unbounded, able to take on any real number value.

Spatiotemporal association levels were modeled as binomially distributed response variables, where the number of reader-night pairs in which one or both mice appeared (i.e., the denominator of SRI for that pair) was the number of trials and the number of reader-night pairs in which both mice appeared (i.e., the numerator for SRI of that pair) was the number of successes. Jaccard index phenotype similarity variables were modeled as beta-distributed response variables with a logit link function. Beta distributions do not contain 0 or 1, whereas it is possible for our similarity scores to be 0 or 1. However, this is vanishingly unlikely to occur (requiring, respectively, that there be no immune cell types in common or the exact same percentages for each cell type across samples with very large numbers of cells), and we thus considered the use of a beta distribution as an appropriate choice instead of a zero-and-one-inflated beta regression (*71*). Manhattan distance phenotype similarity variables were log-transformed and modeled as normally distributed response variables. Manhattan distance increases as the similarity of phenotypes decreases; for ease of understanding, we report all coefficient values for regressions predicting Manhattan distance as their negatives, such that a positive coefficient indicates a correlation with increased similarity for both cell distribution similarity and cytokine production similarity.

Supplementary Materials

This PDF file includes:
Supplementary Text
Figs. S1 to S12
Tables S1 to S10, and S12 to S21
Legend for table S11
References

Other Supplementary Material for this manuscript includes the following:
Table S11

REFERENCE AND NOTES

1. A. Kraus, K. M. Buckley, I. Salinas, Sensing the world and its dangers: An evolutionary perspective in neuroimmunology. *eLife* **10**, e66706 (2021).
2. P. Brodin, M. M. Davis, Human immune system variation. *Nat. Rev. Immunol.* **17**, 21–29 (2017).
3. K. J. Kaczorowski, K. Shekhar, D. Nkulikiyimfura, C. L. Dekker, H. Maecker, M. M. Davis, A. K. Chakraborty, P. Brodin, Continuous immunotypes describe human immune variation and predict diverse responses. *Proc. Natl. Acad. Sci. U.S.A.* **114**, E6097–E6106 (2017).
4. S. Abolins, L. Lazarou, L. Weldon, L. Hughes, E. C. King, P. Drescher, M. J. O. Pocock, J. C. R. Hafalla, E. M. Riley, M. Viney, The ecology of immune state in a wild mammal, *Mus musculus domesticus*. *PLOS Biology* **16**, e2003538 (2018).
5. P. Brodin, V. Jojic, T. Gao, S. Bhattacharya, C. J. L. Angel, D. Furman, S. Shen-Orr, C. L. Dekker, G. E. Swan, A. J. Butte, H. T. Maecker, M. M. Davis, Variation in the human immune system is largely driven by non-heritable influences. *Cell* **160**, 37–47 (2015).
6. B. P. Lazzaro, T. J. Little, Immunity in a variable world. *Philos. Trans. R. Soc. Lond. B. Biol. Sci.* **364**, 15–26 (2009).
7. M. Salathé, M. Kazandjieva, J. W. Lee, P. Levis, M. W. Feldman, J. H. Jones, A high-resolution human contact network for infectious disease transmission. *Proc. Natl. Acad. Sci. U.S.A.* **107**, 22020–22025 (2010).
8. L. A. Meyers, B. Pourbohloul, M. E. J. Newman, D. M. Skowronski, R. C. Brunham, Network theory and SARS: Predicting outbreak diversity. *J. Theor. Biol.* **232**, 71–81 (2005).
9. J. Tung, L. B. Barreiro, M. B. Burns, J.-C. Grenier, J. Lynch, L. E. Grieneisen, J. Altmann, S. C. Alberts, R. Blekhman, E. A. Archie, Social networks predict gut microbiome composition in wild baboons. *eLife* **4**, e05224 (2015).
10. A. C. Perofsky, R. J. Lewis, L. A. Abondano, A. Di Fiore, L. A. Meyers, Hierarchical social networks shape gut microbial composition in wild Verreaux's sifaka. *Proc. Biol. Sci.* **284**, 20172274 (2017).
11. A. Raulo, B. E. Allen, T. Troitsky, A. Husby, J. A. Firth, T. Coulson, S. C. L. Knowles, Social networks strongly predict the gut microbiota of wild mice. *ISME J.* **15**, 2601–2613 (2021).
12. K. Yarlagadda, I. Razik, R. S. Malhi, G. G. Carter, Social convergence of gut microbiomes in vampire bats. *Biol. Lett.* **17**, 20210389 (2021).
13. K. A. Dill-McFarland, Z.-Z. Tang, J. H. Kemis, R. L. Kerby, G. Chen, A. Palloni, T. Sorenson, F. E. Rey, P. Herd, Close social relationships correlate with human gut microbiota composition. *Sci. Rep.* **9**, 703 (2019).
14. A. Sarkar, S. Harty, K. V.-A. Johnson, A. H. Moeller, E. A. Archie, L. D. Schell, R. N. Carmody, T. H. Clutton-Brock, R. I. M. Dunbar, P. W. J. Burnet, Microbial transmission in animal social networks and the social microbiome. *Nat. Ecol. Evol.* **4**, 1020–1035 (2020).
15. G. F. Albery, L. Kirkpatrick, J. A. Firth, S. Bansal, Unifying spatial and social network analysis in disease ecology. *J. Anim. Ecol.* **90**, 45–61 (2021).
16. D. R. Farine, Proximity as a proxy for interactions: Issues of scale in social network analysis. *Anim. Behav.* **104**, e1–e5 (2015).
17. C. C. Vogt, M. N. Zipple, D. D. Sprockett, C. H. Miller, S. X. Hardy, M. K. Arthur, A. M. Greenstein, M. S. Colvin, L. M. Michel, A. H. Moeller, M. J. Sheehan, Spatial and social structure of rewilded laboratory mice. bioRxiv 2022.04.19.488643 (2023); https://doi.org/10.1101/2022.04.19.488643.
18. L. V. Hooper, D. R. Littman, A. J. Macpherson, Interactions between the microbiota and the immune system. *Science* **336**, 1268–1273 (2012).
19. J. Schluter, J. U. Peled, B. P. Taylor, K. A. Markey, M. Smith, Y. Taur, R. Niehus, A. Staffas, A. Dai, E. Fontana, L. A. Amoretti, R. J. Wright, S. Morjaria, M. Fenelus, M. S. Pessin, N. J. Chao, M. Lew, L. Bohannon, A. Bush, A. D. Sung, T. M. Hohl, M.-A. Perales, M. R. M. van den Brink, J. B. Xavier, The gut microbiota is associated with immune cell dynamics in humans. *Nature* **588**, 303–307 (2020).
20. M. P. Spindler, S. Siu, I. Mogno, Z. Li, C. Yang, S. Mehandru, G. J. Britton, J. J. Faith, Human gut microbiota stimulate defined innate immune responses that vary from phylum to strain. *Cell Host Microbe* **30**, 1481–1498.e5 (2022).
21. J. M. Leung, S. A. Budischak, H. C. The, C. Hansen, R. Bowcutt, R. Neill, M. Shellman, P. Loke, A. L. Graham, Rapid environmental effects on gut nematode susceptibility in rewilded mice. *PLOS Biol.* **16**, e2004108 (2018).
22. S. P. Rosshart, J. Herz, B. G. Vassallo, A. Hunter, M. K. Wall, J. H. Badger, J. A. McCulloch, D. G. Anastasakis, A. A. Sarshad, I. Leonardi, N. Collins, J. A. Blatter, S.-J. Han, S. Tamoutounour, S. Potapova, M. B. Foster St, W. Claire, S. K. Yuan, M. S. Sen, B. Dreier, M. Hild, D. Hafner, I. D. Wang, Y. Iliev, G. Belkaid, B. R. Trinchieri, Laboratory mice born to wild mice have natural microbiota and model human immune responses. *Science* **365**, eaaw4361 (2019).
23. J.-D. Lin, J. C. Devlin, F. Yeung, C. McCauley, J. M. Leung, Y.-H. Chen, A. Cronkite, C. Hansen, C. Drake-Dunn, K. V. Ruggles, K. Cadwell, A. L. Graham, P. Loke, Rewilding *Nod2* and *Atg16l1* mutant mice uncovers genetic and environmental contributions to microbial responses and immune cell composition. *Cell Host Microbe* **27**, 830–840.e4 (2020).
24. F. Yeung, Y.-H. Chen, J.-D. Lin, J. M. Leung, C. McCauley, J. C. Devlin, C. Hansen, A. Cronkite, Z. Stephens, C. Drake-Dunn, Y. Fulmer, B. Shopsin, K. V. Ruggles, J. L. Round, P. Loke, A. L. Graham, K. Cadwell, Altered immunity of laboratory mice in the natural environment is associated with fungal colonization. *Cell Host Microbe* **27**, 809–822.e6 (2020).
25. S. P. Rosshart, B. G. Vassallo, D. Angeletti, D. S. Hutchinson, A. P. Morgan, K. Takeda, H. D. Hickman, J. A. McCulloch, J. H. Badger, N. J. Ajami, G. Trinchieri, F. Pardo-Manuel de Villena, J. W. Yewdell, B. Rehermann, Wild mouse gut microbiota promotes host fitness and improves disease resistance. *Cell* **171**, 1015–1028.e13 (2017).
26. Y.-H. Chen, F. Yeung, K. A. Lacey, K. Zaldana, J.-D. Lin, G. C. W. Bee, C. McCauley, R. S. Barre, S.-H. Liang, C. B. Hansen, A. E. Downie, K. Tio, J. N. Weiser, V. J. Torres, R. J. Bennett, P. Loke, A. L. Graham, K. Cadwell, Rewilding of laboratory mice enhances granulopoiesis and immunity through intestinal fungal colonization. *Sci. Immunol.* **8**, eadd6910 (2023).
27. S. E. Hamilton, V. P. Badovinac, L. K. Beura, M. Pierson, S. C. Jameson, D. Masopust, T. S. Griffith, New insights into the immune system using dirty mice. *J. Immunol.* **205**, 3–11 (2020).
28. G. F. Albery, D. J. Becker, F. Kenyon, D. H. Nussey, J. M. Pemberton, The fine-scale landscape of immunity and parasitism in a wild ungulate population. *Integr. Comp. Biol.* **59**, 1165–1175 (2019).
29. P. C. Lopes, E. H. D. Carlitz, M. Kindel, B. König, Immune-endocrine links to gregariousness in wild house mice. *Front. Behav. Neurosci.* **14**, (2020).

30. I. Leonardi, I. H. Gao, W.-Y. Lin, M. Allen, X. V. Li, W. D. Fiers, M. B. De Celie, G. G. Putzel, R. K. Yantiss, M. Johncilla, D. Colak, I. D. Iliev, Mucosal fungi promote gut barrier function and social behavior via Type 17 immunity. *Cell* **185**, 831–846.e14 (2022).
31. A. J. Filiano, Y. Xu, N. J. Tustison, R. L. Marsh, W. Baker, I. Smirnov, C. C. Overall, S. P. Gadani, S. D. Turner, Z. Weng, S. N. Peerzade, H. Chen, K. S. Lee, M. M. Scott, M. P. Beenhakker, V. Litvak, J. Kipnis, Unexpected role of interferon-γ in regulating neuronal connectivity and social behaviour. *Nature* **535**, 425–429 (2016).
32. E. J. Carr, J. Dooley, J. E. Garcia-Perez, V. Lagou, J. C. Lee, C. Wouters, I. Meyts, A. Goris, G. Boeckxstaens, M. A. Linterman, A. Liston, The cellular composition of the human immune system is shaped by age and cohabitation. *Nat. Immunol.* **17**, 461–468 (2016).
33. A. L. Graham, Naturalizing mouse models for immunology. *Nat. Immunol.* **22**, 111–117 (2021).
34. R. W. Logan, R. F. Robledo, J. M. Recla, V. M. Philip, J. A. Bubier, J. J. Jay, C. Harwood, T. Wilcox, D. M. Gatti, C. J. Bult, G. A. Churchill, E. J. Chesler, High-precision genetic mapping of behavioral traits in the diversity outbred mouse population. *Genes Brain Behav.* **12**, 424–437 (2013).
35. M. Loos, B. Koopmans, E. Aarts, G. Maroteaux, S. van der Sluis, N.-B. S. I. K. M. P. Consortium, M. Verhage, A. B. Smit, Sheltering behavior and locomotor activity in 11 genetically diverse common inbred mouse strains using home-cage monitoring. *PLOS ONE* **9**, e108563 (2014).
36. O. Oyesola, A. E. Downie, N. Howard, R. S. Barre, K. Kiwanuka, K. Zaldana, Y.-H. Chen, A. Menezes, S. C. Lee, J. Devlin, O. Mondragón-Palomino, C. O. S. Souza, C. Herrmann, S. B. Koralov, K. Cadwell, A. L. Graham, P. Loke, Genetic and Environmental interactions contribute to immune variation in rewilded mice. bioRxiv 2023.03.17.533121 (2023); https://doi.org/10.1101/2023.03.17.533121.
37. D. R. Farine, H. Whitehead, Constructing, conducting and interpreting animal social network analysis. *J. Anim. Ecol.* **84**, 1144–1163 (2015).
38. S. J. Cairns, S. J. Schwager, A comparison of association indices. *Anim. Behav.* **35**, 1454–1469 (1987).
39. M. E. J. Newman, Mixing patterns in networks. *Phys. Rev. E* **67**, 026126 (2003).
40. T. Ren, S. Boutin, M. M. Humphries, B. Dantzer, J. C. Gorrell, D. W. Coltman, A. G. McAdam, M. Wu, Seasonal, spatial, and maternal effects on gut microbiome in wild red squirrels. *Microbiome* **5**, 163 (2017).
41. D. J. Becker, G. F. Albery, M. K. Kessler, T. J. Lunn, C. A. Falvo, G. Á. Czirják, L. B. Martin, R. K. Plowright, Macroimmunology: The drivers and consequences of spatial patterns in wildlife immune defence. *J. Anim. Ecol.* **89**, 972–995 (2020).
42. S. A. Budischak, C. B. Hansen, Q. Caudron, R. Garnier, T. R. Kartzinel, I. Pelczer, C. E. Cressler, A. van Leeuwen, A. L. Graham, Feeding immunity: Physiological and behavioral responses to infection and resource limitation. *Front. Immunol.* **8**, 01914 (2018).
43. C. H. Taylor, S. Young, J. Fenn, A. L. Lamb, A. E. Lowe, B. Poulin, A. D. C. MacColl, J. E. Bradley, Immune state is associated with natural dietary variation in wild mice *Mus musculus domesticus*. *Funct. Ecol.* **33**, 1425–1435 (2019).
44. T. O. Richardson, T. E. Gorochowski, Beyond contact-based transmission networks: The role of spatial coincidence. *J. R. Soc. Interface.* **12**, 20150705 (2015).
45. R. Poretsky, L. M. Rodriguez-R, C. Luo, D. Tsementzi, K. T. Konstantinidis, Strengths and limitations of 16S rRNA gene amplicon sequencing in revealing temporal microbial community dynamics. *PLOS ONE* **9**, e93827 (2014).
46. E. van Tilburg Bernardes, V. K. Pettersen, M. W. Gutierrez, I. Laforest-Lapointe, N. G. Jendzjowsky, J.-B. Cavin, F. A. Vicentini, C. M. Keenan, H. R. Ramay, J. Samara, W. K. MacNaughton, R. J. A. Wilson, M. M. Kelly, K. D. McCoy, K. A. Sharkey, M.-C. Arrieta, Intestinal fungi are causally implicated in microbiome assembly and immune development in mice. *Nat. Commun.* **11**, 2577 (2020).
47. A. C. Love, K. Grisham, J. B. Krall, C. G. Goodchild, S. E. DuRant, Perception of infection: Disease-related social cues influence immunity in songbirds. *Biol. Lett.* **17**, 20210125 (2021).
48. V. Bocci, Interleukins. *Clin. Pharmacokinet.* **21**, 274–284 (1991).
49. G. Altan-Bonnet, R. Mukherjee, Cytokine-mediated communication: A quantitative appraisal of immune complexity. *Nat. Rev. Immunol.* **19**, 205–217 (2019).
50. J. J. C. Thome, N. Yudanin, Y. Ohmura, M. Kubota, B. Grinshpun, T. Sathaliyawala, T. Kato, H. Lerner, Y. Shen, D. L. Farber, Spatial map of human T cell compartmentalization and maintenance over decades of life. *Cell* **159**, 814–828 (2014).
51. M. Lee, J. N. Mandl, R. N. Germain, A. J. Yates, The race for the prize: T-cell trafficking strategies for optimal surveillance. *Blood* **120**, 1432–1438 (2012).
52. N. Snyder-Mackler, J. Sanz, J. N. Kohn, J. F. Brinkworth, S. Morrow, A. O. Shaver, J.-C. Grenier, R. Pique-Regi, Z. P. Johnson, M. E. Wilson, L. B. Barreiro, J. Tung, Social status alters immune regulation and response to infection in macaques. *Science* **354**, 1041–1045 (2016).
53. A. J. Lea, M. Y. Akinyi, R. Nyakundi, P. Mareri, F. Nyundo, T. Kariuki, S. C. Alberts, E. A. Archie, J. Tung, Dominance rank-associated gene expression is widespread, sex-specific, and a precursor to high social status in wild male baboons. *Proc. Natl. Acad. Sci. U.S.A.* **115**, E12163–E12171 (2018).
54. J. A. Anderson, A. J. Lea, T. N. Voyles, M. Y. Akinyi, R. Nyakundi, L. Ochola, M. Omondi, F. Nyundo, Y. Zhang, F. A. Campos, S. C. Alberts, E. A. Archie, J. Tung, Distinct gene regulatory signatures of dominance rank and social bond strength in wild baboons. *Philos. Trans. R. Soc. Lond. B. Biol. Sci.* **377**, 20200441 (2022).
55. W. Lee, T. M. Milewski, M. F. Dwortz, R. L. Young, A. D. Gaudet, L. K. Fonken, F. A. Champagne, J. P. Curley, Distinct immune and transcriptomic profiles in dominant versus subordinate males in mouse social hierarchies. *Brain Behav. Immun.* **103**, 130–144 (2022).
56. N. Geva-Zatorsky, D. Alvarez, J. E. Hudak, N. C. Reading, D. Erturk-Hasdemir, S. Dasgupta, U. H. von Andrian, D. L. Kasper, In vivo imaging and tracking of host–microbiota interactions via metabolic labeling of gut anaerobic bacteria. *Nat. Med.* **21**, 1091–1100 (2015).
57. J. Freund, A. M. Brandmaier, L. Lewejohann, I. Kirste, M. Kritzler, A. Krüger, N. Sachser, U. Lindenberger, G. Kempermann, Emergence of individuality in genetically identical mice. *Science* **340**, 756–759 (2013).
58. G. Dwyer, J. S. Elkinton, J. P. Buonaccorsi, Host heterogeneity in susceptibility and disease dynamics: Tests of a mathematical model. *Am. Nat.* **150**, 685–707 (1997).
59. A. E. Fleming-Davies, V. Dukic, V. Andreasen, G. Dwyer, Effects of host heterogeneity on pathogen diversity and evolution. *Ecol. Lett.* **18**, 1252–1261 (2015).
60. V. M. Link, S. H. Duttke, H. B. Chun, I. R. Holtman, E. Westin, M. A. Hoeksema, Y. Abe, D. Skola, C. E. Romanoski, J. Tao, G. J. Fonseca, T. D. Troutman, N. J. Spann, T. Strid, M. Sakai, M. Yu, R. Hu, R. Fang, D. Metzler, B. Ren, C. K. Glass, Analysis of genetically diverse macrophages reveals local and domain-wide mechanisms that control transcription factor binding and function. *Cell* **173**, 1796–1809.e17 (2018).
61. A. J. Lusis, M. M. Seldin, H. Allayee, B. J. Bennett, M. Civelek, R. C. Davis, E. Eskin, C. R. Farber, S. Hui, M. Mehrabian, F. Norheim, C. Pan, B. Parks, C. D. Rau, D. J. Smith, T. Vallim, Y. Wang, J. Wang, The hybrid mouse diversity panel: A resource for systems genetics analyses of metabolic and cardiovascular traits. *J. Lipid Res.* **57**, 925–942 (2016).
62. P.-C. Bürkner, brms: An R Package for Bayesian Multilevel Models Using Stan. *J. Stat. Softw.* **80**, 1–28 (2017).
63. P.-C. Bürkner, J. Gabry, S. Weber, A. Johnson, M. Modrak, H. S. Badr, F. Weber, M. S. Ben-Shachar, H. Rabel, S. C. Mills, brms: Bayesian Regression Models using "Stan," version 2.18.0 (2022); https://CRAN.R-project.org/package=brms.
64. J. Oksanen, G. L. Simpson, F. G. Blanchet, R. Kindt, P. Legendre, P. R. Minchin, R. B. O'Hara, P. Solymos, M. H. H. Stevens, E. Szoecs, H. Wagner, M. Barbour, M. Bedward, B. Bolker, D. Borcard, G. Carvalho, M. Chirico, M. D. Caceres, S. Durand, H. B. A. Evangelista, R. FitzJohn, M. Friendly, B. Furneaux, G. Hannigan, M. O. Hill, L. Lahti, D. McGlinn, M.-H. Ouellette, E. R. Cunha, T. Smith, A. Stier, C. J. F. T. Braak, J. Weedon, vegan: Community Ecology Package, version 2.6-4 (2022); https://CRAN.R-project.org/package=vegan.
65. D. R. Farine, A guide to null models for animal social network analysis. *Methods Ecol. Evol.* **8**, 1309–1320 (2017).
66. D. W. Franks, M. N. Weiss, M. J. Silk, R. J. Y. Perryman, D. P. Croft, Calculating effect sizes in animal social network analysis. *Methods Ecol. Evol.* **12**, 33–41 (2021).
67. I. Puga-Gonzalez, C. Sueur, S. Sosa, Null models for animal social network analysis and data collected via focal sampling: Pre-network or node network permutation? *Methods Ecol. Evol.* **12**, 22–32 (2021).
68. M. N. Weiss, D. W. Franks, L. J. N. Brent, S. Ellis, M. J. Silk, D. P. Croft, Common datastream permutations of animal social network data are not appropriate for hypothesis testing using regression models. *Methods Ecol. Evol.* **12**, 255–265 (2021).
69. D. R. Farine, G. G. Carter, Permutation tests for hypothesis testing with animal social network data: Problems and potential solutions. *Methods Ecol. Evol.* **13**, 144–156 (2022).
70. J. D. A. Hart, M. N. Weiss, L. J. N. Brent, D. W. Franks, Common permutation methods in animal social network analysis do not control for non-independence. *Behav. Ecol. Sociobiol.* **76**, 151 (2022).
71. J. C. Douma, J. T. Weedon, Analysing continuous proportions in ecology and evolution: A practical introduction to beta and Dirichlet regression. *Methods Ecol. Evol.* **10**, 1412–1430 (2019).
72. F. H. Bronson, The reproductive ecology of the house mouse. *Q. Rev. Biol.* **54**, 265–299 (1979).
73. K. L. Svenson, B. Paigen, Recommended housing densities for research mice: Filling the gap in data-driven alternatives. *FASEB J.* **33**, 3097–3111 (2019).
74. D. G. Mikesic, L. C. Drickamer, Factors affecting home-range size in house mice (*Mus musculus domesticus*) living in outdoor enclosures. *Am. Midl. Nat.* **127**, 31–40 (1992).

Acknowledgments: We thank W. Craigens, C. Hansen, and the Graham Lab for invaluable assistance in the field. In addition, we thank M. Zhao for help with setting up experiments in the lab and J. Devlin and J. Randall for help in maintaining the Joes' Flow App Software. We thank E. T. Wojno for providing the *T. muris* parasite larvae. We thank A. Raulo, S. Knowles, the Knowles Lab, R. Froemke, S. Naik, and W. Gause for comments and suggestions. **Funding:** This work was supported by the National Science Foundation, award no. DGE-2039656 (A.E.D.); Division of Intramural Research, National Institute of Allergy and Infectious Diseases, National Institutes of

Health (NIH) (P.L.); and New Jersey Alliance for Clinical and Translational Science (NJ ACTS; New Jersey Health Foundation Inc., in collaboration with a Clinical and Translational Science Award from the National Center for Advancing Translational Science of the NIH), award no. UL1TR003017 (A.L.G.). This publication was supported by the Princeton University Library Open Access Fund. The content is solely the responsibility of the authors and does not represent the official views of the NIH. **Author contributions:** Conceptualization: A.E.D., O.O., K.C., P.L., and A.L.G. Methodology: A.E.D., O.O., Q.C., Y.-H.C., E.J.D., R.G., K.K., D.J.N., C.K.T., O.M.-P., and A.L.G. Investigation: A.E.D., O.O., R.S.B., Y.-H.C., K.K., A.M., O.M.-P., K.Z., P.L., and A.L.G. Data curation and analysis: A.E.D., O.O., and A.L.G. Hardware and software: A.E.D., Q.C., R.G., and J.B.S. Writing—original draft: A.E.D., O.O., P.L., and A.L.G. Writing—review and editing: A.E.D., O.O., E.J.D., A.M., C.K.T., K.C., P.L., and A.L.G. Visualization: A.E.D., O.O., and A.L.G. Supervision: K.C., P.L., and A.L.G. Funding acquisition: K.C., P.L., and A.L.G. All authors read and approved the final manuscript. **Competing interests:** K.C. has received research funding from Pfizer, Takeda, Pacific Biosciences, Genentech, and Abbvie, and P.L. has received research funding from Pfizer. K.C. has consulted for or received an honorarium from Puretech Health, Genentech, and Abbvie. K.C. is an inventor on US patent 10,722,600 and provisional patents 62/935,035 and 63/157,225. P.L. is a federal employee. The other authors declare that they have no competing interests. **Data and materials availability:** All data needed to evaluate the conclusions in the paper are present in the paper and/or the Supplementary Materials. All metadata, behavioral data, immunological data, and analysis code are available at https://doi.org/10.5061/dryad.rjdfn2zjc and https://github.com/aedownie/rewilding2021.

Submitted 16 March 2023
Accepted 21 November 2023
Published 22 December 2023
10.1126/sciadv.adh8310